PROCEEDINGS OF SCIENCE

A parton shower consistent with parton densities at LO and NLO: PDF2ISR

Hannes Jung,[a,b] **Leif Lönnblad,**[c] **Mikel Mendizabal**[a,*] **and Sara Taheri Monfared**[a]

[a] *Deutsches Elektronen-Synchrotron DESY, Germany*
[b] *II. Institut fur Theoretische Physik, Universitat Hamburg, Hamburg, Germany*
[c] *Department of Physics, Lund University, Lund, Sweden*

E-mail: mikel.mendizabal.morentin@desy.de

We present a method for obtaining an initial-state parton shower model where the (backward) evolution is fully consistent with the (forward) evolution of the collinear parton density is used. As a proof-of-concept we use parton densities obtained with the Parton Branching (PB) approach, and modify the default initial-state shower in PYTHIA8 with this method for consistency. PB is ideally suited for checking the validity of our method since, in addition to producing collinear parton densities, it also produces the corresponding transverse dependent (TMD) ones, and these can then be directly compared to the transverse momentum distribution obtained from the parton shower. We show that TMD distributions which we in this way obtain from our modified PYTHIA8 shower using leading order (LO) parton densities and splitting functions are fully consistent with the corresponding leading order TMD densities. At next-to-leading order (NLO) it is not possible to achieve the same consistency using the built-in LO splitting functions in the shower, but we show that by introducing NLO splitting functions using a reweighting procedure, we can achieve consistency also at NLO. The method presented here, which we have named PDF2ISR, can be easily extended to any collinear parton densities, as long as the exact conditions for the evolution are known. With the PDF2ISR method we obtain an initial-state parton shower which in principle has no free parameters, and is fully consistent with collinear parton densities at LO and NLO.

QCD at the Extremes (QCDEX2025)
1–5 Sept 2025
Online

*Speaker

 ISSN 1824-8039 . Published by SISSA Medialab.

PoS(QCDEX2025)005

1. Introduction

The description of particle collisions is a hard task, as many different processes and energy scales are present, from the hard partonic interaction, multiple partonic interactions, hadrons and their fragmentation and multiple emissions. For this, fixed order calculations are not enough for most cases and need to be supplemented for example with multi purpose Monte Carlo Event Generators (MCEG), which take care of describing the different processes involved in particle collisions.

In these collisions more than one energy scales can appear, the hard scale, Q and a secondary scale, ν. In the presence of a secondary scale logarithms of the type $\ln \nu^2/Q^2$ arise, and these become large when $\nu \ll Q$. To achieve a physical description these logarithms need to be resummed to all orders. The transverse momentum of a colour singlet boson, q_T, produced in proton-proton collisions is the most studied process, where $\nu = q_T$. In this process these large logarithms are produced by multiple gluon emissions and thus these gluons emissions are to be resummed to all orders.

Different prescriptions exist for the soft gluon resummation and the description of the transverse momentum spectrum of electroweak boson: TMD factorisation, SCET, parton showers, Parton Branching, etc. In this work we focus on parton showers, precisely in the initial state shower, a core element of MCEG. The evolution in parton-showers is governed by the Sudakov form factor [1, 2]:

$$\Delta_a = \exp - \sum_b \int_{\mu_0^2}^{Q^2} \frac{d\mu'^2}{\mu'^2} \int_0^1 dz z P_{ab}^{(R)}(z, \mu^2), \tag{1}$$

which represents the probability of no emission, where z is the momentum transfer from parton a to b, μ' is the scale of the branching and $P_{ab}^{(R)}$ are the real emission DGLAP evolution kernels. The initial state shower is based on the backward evolution, it starts from the hard-scale of the process, Q, and evolves backwards to the initial scale μ_0, and thus the Sudakov form factor is modified,

$$\Delta_a^{\text{Backward}} = \exp - \sum_b \int_{\mu_{i-1}^2}^{Q^2} \frac{d\mu'^2}{\mu'^2} \int_x^{z_{dyn}} dz P_{ab}^{(R)}(z, \mu'^2) \frac{x' f_b(x', \mu')}{x f_a(x, \mu')}, \tag{2}$$

to follow the PDF which was used in the event generation, f_a. While in this way the parton shower is able to reproduce the PDF many inconsistencies are present between the evolution of the PDF and the parton shower backward evolution. In this work we remove these differences and develop a method to create a consistent ISR evolution with the PDF evolution, called PDF2ISR [3]. For that, we compare the Pythia8 ISR [4] to the Parton Branching evolution [1, 2].

2. Parton Branching method

The Parton Branching method allows for the solution of the DGLAP evolution equations. The evolution of a momentum weighted PDF, $x f(x, \mu^2)$ is defined as:

$$\frac{\partial x f_a(x, \mu^2)}{\partial \ln \mu^2} = \sum_b \int_x^1 dz P_{ab}(z, \alpha_s) \frac{x}{z} f_b(x/z, \mu^2) \tag{3}$$

where x is the momentum fraction, P_{ab} is the splitting function for parton b splitting into parton a and z is the momentum transfer from parton b to a. To solve the differential equation iteratively we

can rewrite it in terms of the Sudakov form factor in eq. (1):

$$x f_a(x,\mu^2) = \Delta_a(\mu^2) x f_a(x,\mu_0^2) + \sum_b \int_{\mu_0^2}^{\mu^2} \frac{d\mu'^2}{\mu'^2} \frac{\Delta_a(\mu^2)}{\Delta_a(\mu'^2)} \int_x^{z_{\rm Max}} dz P_{ab}^{(R)}(z,\alpha_s) \frac{x}{z} f_b(x/z,\mu'^2) \quad (4)$$

where $z_{\rm Max} = 1-\epsilon$ and $\epsilon \ll 1$, to avoid the pole at $z \to 1$ in gluon emissions. In the DGLAP evolution the scale μ does not have a physical interpretation. By applying an ordering condition to the emissions we are able to attach a physical meaning to it. The PB method implements the angular ordering condition, which relates the evolution scale with the polar angle and the transverse momentum of the emitted parton, $q_t = (1-z)\mu'$.

Another important aspect of the PB evolution is the scale choice in α_s, a different choice of scale gives rise to different PDF and TMD sets. By obeying the angular ordering condition we get $\alpha_s(q_t) = \alpha_s((1-z)\mu')$. With this definition q_t can reach non-perturbative values, $q_t < 1$ GeV, leading to instabilities in the perturbative calculation. For that, a minimum q_t, $q_{\rm cut} = 1$ GeV, is introduced where α_s is frozen to $\alpha_s(q_{\rm cut})$ for $q_t < q_{\rm cut}$ values. Another option is using directly μ' as scale choice in α_s, $\alpha_s(\mu')$. By fitting the collinear PDFs to HERA data [5], the $\alpha_s(\mu')$ gives rise to the PB-NLO-HERAI+II-2018-set1 collinear and TMD PDFs, while the $\alpha_s(q_t)$ choice to the PB-NLO-HERAI+II-2018-set2 collinear and TMD PDFs [6].

2.1 Pythia8 and Parton Branching differences

Now we shortly introduce the main differences between the Pythia8 backward evolution and the PB evolution. The PB evolution implements up to NLO splitting functions, while Pythia8 only implements LO splitting functions. As previously mentioned in the PB evolution emissions are ordered according to the angular ordering condition, while in Pythia8 according to p_t-ordering, which relates the evolution scale directly to the transverse momentum of the emitted parton, $\mu' = q_t$. These differences in the definition of the transverse momentum of the emitted parton, lead to emissions with larger q_t in the Pythia8 evolution. The evolution in Pythia8 is also based in the resolvability of the emissions, where a dynamical resolution parameter is introduced, $z_{\rm dyn}$, to only take into account resolvable splittings. This leads to a reduction of the emission phase space in the case of Pythia8 ($0 < z < z_{\rm dyn}$) while the PB evolution allows for the whole z range. We have summarised the differences in table 1.

3. The PDF2ISR method

To compare the PB evolution with the Pythia8 ISR we make use of the method developed in [7], the ISR2TMD method. This method allows for the extraction of TMDs from ISR evolution. In a first step we generate events with Pythia8 using the PB-NLO-HERAI+II-2018-set1 collinear PDF and perform the Pythia8 ISR evolution with the CUET tune [8] , to extract the TMD using the ISR2TMD method, TMD-Pythia8-CUET. In figure 1 we compare the extracted TMD with the PB-NLO-HERAI+II-2018-set1 TMD PDF at different x and μ values. We observe large differences between the two TMDs. The TMD generated from the Pythia8 backward evolution shows emissions with larger transverse momentum and a flat behaviour at small k_t, while for the PB-TMD the gluon contribution continues to rise. Thus, even if the Sudakov form factor in the backward evolution

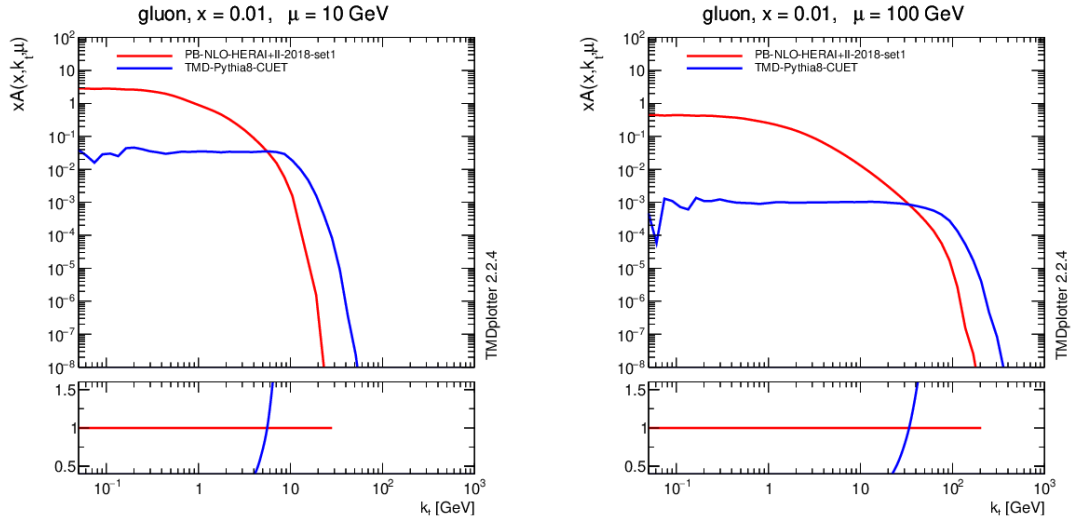

Figure 1: Comparison of the gluon TMD PDF between the PB-NLO-HERAI+II-2018-set1 TMD PDF at NLO in QCD (red), and the gluon TMD extracted from Pythia8 ISR, TMD-Pythia8-CUET (blue) for a momentum fraction $x = 0.01$ at two different scales: 10 GeV (left panel) and 100 GeV (right panel). Figures taken from [3].

	Pythia8	**PB method**
Ordering	$\mu_i^2 = q_{\perp,i}^2$	$q_{\perp,i}^2 = (1-z)^2\mu_i^2$
Phase space	$0 < z < z_{dyn}^{P8}$	$0 < z < z_{\text{Max}}$
Splitting Functions	LO	NLO
α_s treatment	PDG param.	QCDNum num.

Table 1: Differences between the Pythia8 backward evolution and the forward evolution in the PB method.

in eq. 2 accounts for the collinear PDF, the backward evolution in Pythia8 does not match the evolution of the collinear PDF used for the event generation, leading to large differences. In this section we develop the PDF2ISR method, which will allow us to match the forward evolution used in the collinear PDF with the backward evolution of the shower.

3.1 The leading order case

In a first step, we compare the two approaches at leading order and at fixed α_s value of 0.130. We modify the ordering of the backward evolution from p_T-ordering to angular ordering. We remove the dynamical resolution scale, z_{dyn}, matching the phases space of the PB evolution. To do this, new PB collinear and TMD PDFs are calculated. We use the PB-NLO-2018-Set2 starting distribution and evolve the collinear and TMDs according to the aforementioned evolution setup. We refer to this toy collinear PDF as PB-LO-ToySet2-asfixed_0130 and the toy TMD PDF PBTMD-LO-ToySet2-asfixed_0130. We generate events according to the PB-LO-ToySet2-asfixed_0130 collinear PDF and evolve with the new backward evolution obtaining the TMD-Pythia8-PBLO-ToySet2-asfixed_0130 TMD PDF. In figure 2 we compare the two TMD distributions, PBTMD-LO-ToySet2-asfixed_0130

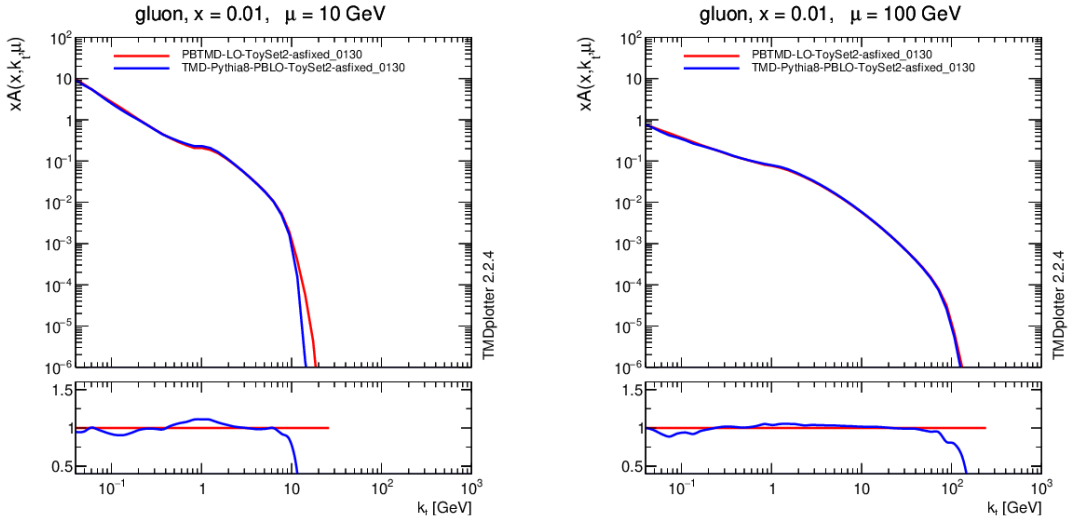

Figure 2: Comparison of the gluon TMD PDF between the PBTMD-LO-ToySet2-asfixed_0130 at LO in QCD (red) and the TMD extracted from PDF2ISR at LO in QCD, TMD-Pythia8-PBLO-ToySet2-asfixed_0130 (blue), for a fixed value of $\alpha_s = 0.130$ and momentum fraction $x = 0.01$ at two different scales: 10 GeV (left panel) and 100 GeV (right panel). Figures taken from [3].

(red line) and TMD-Pythia8-PBLO-ToySet2-asfixed_0130 (blue), we observe that Pythia8, with the modified backward evolution, is able to reproduce the PBTMD-LO-ToySet2-asfixed_0130 TMD PDF in most of the k_t range. We will refer to the modified backward evolution as the PDF2ISR.

To asses the differences in the kinematics of the emission we compute for each splitting the momentum transfer, z, and the transverse momentum, q_T. In figure 3 We show the case of a the evolution of gluons only allowing for $g \to gg$ type of radiations for both PDF2ISR and uPDFevolv2 [9], the code used by PB for the evolution of collinear and TMD PDFs. In both cases the forward and backward evolution show a good agreement for z and q_t.

3.2 The next-to leading order case

At NLO, besides the splitting functions, the treatment of α_s in the evolution code is of importance. As previously shown in table 1 Pythia8 uses the PDG parametrisation of α_s, while the PB evolution, which uses the uPDFevolv2 evolution code, uses the numerical integration used in QCDnum evolution package [10]. At small scales the PDG parametrisation and the QCDNum implementation do not agree. To be consistent, we apply the QCDnum α_s calculation in the PDF2ISR method.

The NLO splitting functions can become negative and thus, lose the probabilistic interpretation we need to generate emissions. In order to overcome this problem, we make use of the LO splitting functions to generate emissions and implement the NLO splitting functions with an extra veto algorithm. The veto algorithm will accept/reject emissions and generate an event weight. While the weight given by the accepted emissions will correct the real emissions, the weight coming from rejected emissions will correctly account for virtual emissions in the Sudakov form factor [11, 12]. We generate events using the PB-NLO-HERAI+II-2018-set1 collinear PDF and shower with the

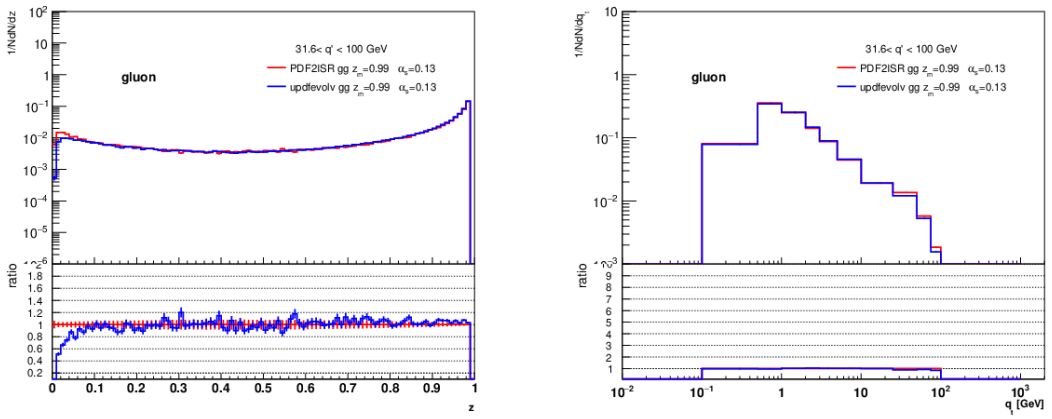

Figure 3: Comparison between forward evolution implemented in the uPDFevolv package (blue) and the PDF2ISR backward evolution (red), for the case of a gluon only allowing to radiate gluons, for a fixed value of $\alpha_s = 0.130$ at LO QCD accuracy for two different kinematic variables: momentum transfer, z (left panel); transverse momentum of the splitting, q_t (right panel). Figures taken from [3].

PDF2ISR evolution with two different scenarios: one with LO splitting functions and another with the NLO splitting functions. In figure 4 we compare the PB-NLO-HERAI+II-2018-set1 TMD PDF (red) with the PDF2ISR evolution with LO splitting functions, TMD-Pythia8-PBNLO-Set1-qs_0.5-LOSplitt (violet), and the PDF2ISR evolution with NLO splitting functions, TMD-Pythia8-PBNLO-Set1-NLOHook (blue). We observe that the PDF2ISR case with only LO splitting functions does not show a good agreement with the PB TMD, but once the NLO splitting functions are implemented the PDF2ISR method agrees remarkably. This shows that the backward evolution of a parton shower can be matched to the collinear PDF used in the event generation, not only respecting the collinear distribution but also the kinematics of each splitting.

4. Conclusion

In MCEG events are generated according to a collinear PDF and to account for soft gluon emissions in the initial state, each incoming parton is evolved backwards. The backward evolution accounts for the collinear PDF by modifying the Sudakov form factor but the kinematics of each emission largely differ from the evolution of forward evolution of the collinear PDF. The emission phase space, the QCD order of the splitting functions and the ordering variable, among other factors, do not match, generating completely different kinematics of each radiation in the collinear PDF evolution and the parton shower.

In this work we have introduced a new method to derive a parton shower consistent with the collinear PDF used in the event generation. We have modified the emission phase space and the evolution ordering according to the collinear PDF. To account for higher order splitting functions we have implemented an extra veto algorithm which correctly incorporates real and virtual

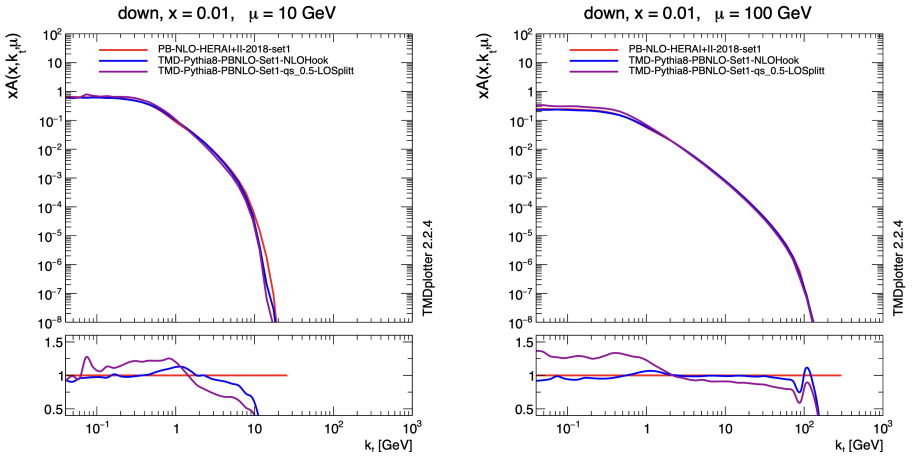

Figure 4: Comparison of the down quark TMD PDF between the PB TMD at NLO in QCD, PB-NLO-HERAI+II-2018-set1 (red); the TMD extracted from PDF2ISR at NLO in QCD, TMD-Pythia8-PBNLO-Set1-NLOHook (blue); and the TMD extracted from PDF2ISR with LO splitting functions, TMD-Pythia8-PBNLO-Set1-qs_0.5-LOSplitt (purple) for momentum fraction $x = 0.01$ at two different scales: 10 GeV (left panel) and 100 GeV (right panel) [3].

contributions. This new method, the PDF2ISR method, is universal, which is valid for any collinear PDF once the details of the evolution are known. Exploiting the extra veto algorithm the method could be extended to NNLO accuracy in QCD. In conclusion, the PDF2ISR method allows for a correct matching between the evolution of the collinear PDF and the backward evolution of the MCEG.

References

[1] F. Hautmann, H. Jung, A. Lelek, V. Radescu, and R. Zlebcik. Soft-gluon resolution scale in QCD evolution equations. *Phys. Lett. B*, 772:446–451, 2017.

[2] F. Hautmann, H. Jung, A. Lelek, V. Radescu, and R. Zlebcik. Collinear and TMD Quark and Gluon Densities from Parton Branching Solution of QCD Evolution Equations. *JHEP*, 01:070, 2018.

[3] H. Jung, L. Lönnblad, M. Mendizabal, and Sara Taheri Monfared. A parton shower consistent with parton densities at LO and NLO: Pdf2Isr. *Eur. Phys. J. C*, 85(8):870, 2025.

[4] Christian Bierlich et al. A comprehensive guide to the physics and usage of PYTHIA 8.3. *SciPost Phys. Codeb.*, 2022:8, 2022.

[5] H. Abramowicz et al. Combination of measurements of inclusive deep inelastic $e^{\pm}p$ scattering cross sections and QCD analysis of HERA data. *Eur. Phys. J. C*, 75(12):580, 2015.

[6] A. Bermudez Martinez, P. Connor, H. Jung, A. Lelek, R. Žlebčík, F. Hautmann, and V. Radescu. Collinear and TMD parton densities from fits to precision DIS measurements in the parton branching method. *Phys. Rev. D*, 99(7):074008, 2019.

[7] H. Jung, S. Steel, S. Taheri Monfared, and Y. Zhou. *TMDs from Monte Carlo event generators*. 12 2021.

[8] Vardan Khachatryan et al. Event generator tunes obtained from underlying event and multi-parton scattering measurements. *Eur. Phys. J. C*, 76(3):155, 2016.

[9] H. Jung, A. Lelek, K. Moral Figueroa, and S. Taheri Monfared. The Parton Branching evolution package uPDFevolv2. 5 2024.

[10] M. Botje. QCDNUM: Fast QCD Evolution and Convolution. *Comput. Phys. Commun.*, 182:490–532, 2011.

[11] Leif Lönnblad. Fooling Around with the Sudakov Veto Algorithm. *Eur. Phys. J. C*, 73(3):2350, 2013.

[12] S. Mrenna and P. Skands. Automated Parton-Shower Variations in Pythia 8. *Phys. Rev. D*, 94(7):074005, 2016.